REPORT DOCUMENTATION PAGE

Form Approved
OMB NO. 0704-0188

1. AGENCY USE ONLY (Leave Blank)	2. REPORT DATE 11/22/2000	3. REPORT TYPE AND DATES COVERED Final Report 07/01/1999 to 07/01/2000

4. TITLE AND SUBTITLE

Rigorous Electromagnetic Analysis of Uncooled Microbolometer

5. FUNDING NUMBERS

DAAD19-99-1-0255

6. AUTHOR(S)
Mark S. Mirotznik

7. PERFORMING ORGANIZATION NAME(S) AND ADDRESS(ES)

The Catholic University of America, 620 Michigan Ave
Washington D.C., 20064

8. PERFORMING ORGANIZATION REPORT NUMBER

9. SPONSORING / MONITORING AGENCY NAME(S) AND ADDRESS(ES)

U. S. Army Research Office
P.O. Box 12211
Research Triangle Park, NC 27709-2211

10. SPONSORING / MONITORING AGENCY REPORT NUMBER

ARO 40127.1-PH

11. SUPPLEMENTARY NOTES

The views, opinions and/or findings contained in this report are those of the author(s) and should not be construed as an official Department of the Army position, policy or decision, unless so designated by other documentation.

12 a. DISTRIBUTION / AVAILABILITY STATEMENT	12 b. DISTRIBUTION CODE
Approved for public release; distribution unlimited.	

13. ABSTRACT (Maximum 200 words)

The specific goal of this project was to develop a rigorous three dimensional electromagnetic model of an uncooled microbolometer array. The optical absorption of the thin-film thermal infrared detector was calculated as a function of wavelength, pixel size, incident angle and area fill factor using the finite-difference-time-domain (FDTD) method. The results indicate that smaller pixels absorb a significantly higher percentage of incident energy than larger pixels with the same fill factor. A polynomial approximation to the FDTD results was derived for use in system models.This model can then be used to analyze the coupling efficiency of the bolometer array as a function of various structural and source variations. These include varying the pixel pitch, fill factor and incident field wavelength and incident angle.

Most Significant Findings:
1) The optical coupling efficiency of microbolometers varies as a complex function of the pixel pitch and fill factor.
2) Due to small pixel diffraction effects the coupling efficiency actually improves as the pixel size is reduced
3) There is an optimal combination of pixel pitch and fill factor that will maximize the coupling efficiency
4) The optical coupling is not sensitive to small variations in incident angle (<45 degrees)

14. SUBJECT TERMS microbolometers, optical absorption, finite difference time domain (FDTD), rigorous electromagnetic analysis			15. NUMBER OF PAGES 16. PRICE CODE
17. SECURITY CLASSIFICATION OF REPORT **UNCLASSIFIED**	18. SECURITY CLASSIFICATION ON THIS PAGE **UNCLASSIFIED**	19. SECURITY CLASSIFICATION OF ABSTRACT **UNCLASSIFIED**	20. LIMITATION OF ABSTRACT **UL**

NSN 7540-01-280-5500 **Standard Form 298**
(Rev.2-89)
Prescribed by ANSI Std. 239-18 298-102

GENERAL INSTRUCTIONS FOR COMPLETING SF 298

The Report Documentation Page (RDP) is used for announcing and cataloging reports. It is important that this information be consistent with the rest of the report, particularly the cover and title page. Instructions for filling in each block of the form follow. It is important to ***stay within the lines*** to meet ***optical scanning requirements.***

Rigorous Electromagnetic Analysis of Uncooled Microbolometer

I. Problem Statement

In the last decade, thermal infrared detectors that are operated near room temperature have made large advances in performance, so that they are now used in, or being considered for, a wide range of commercial and military applications. Thermal detectors work by converting incident infrared radiation to heat, thereby increasing the temperature of the detector. The change in temperature is typically measured as a change in detector resistance (for bolometers) or in the spontaneous polarization across the detector (for ferroelectrics).

For best performance, the detector should have the highest possible absorption, lowest possible thermal conductance between the detector and its surroundings, and a thermal time constant roughly equal to the frame rate. These requirements are sometimes incompatible. For example, if the thermal conductance is reduced without also reducing the detector mass, the thermal time constant becomes too long. Therefore, further improvements in sensitivity will require reductions in thermal conductance *and* mass while maintaining high absorption.

There is also a trend to reduce pixel size in order to improve image resolution. However, as pixel sizes shrink to only a couple of optical wavelengths of the incident radiation, it is unclear how diffraction will effect optical absorption. To investigate small pixel effects it is necessary to employ a rigorous three-dimensional electromagnetic model. In this project, we used the finite-difference time-domain (FDTD) method to compute absorption in finite size pixels placed within an infinitely periodic imaging array. The model was used to determine the fractional absorption as a function of wavelength, determine the effect of fill-factor and pixel size on absorption, and was used to compute an image performance model function.

II. Physical Detector Model and Parameters

Figure 1 shows a typical thermal detector. The design uses a quarter-wavelength cavity [1, 2] to achieve high absorption in a thin, low-mass structure. The ideal form of the quarter-wavelength structure is an infinite conducting film with sheet resistivity equal to the free-space impedance $Z_0 = 120\pi\ \Omega$, spaced one-fourth of a wavelength ($\lambda/4$) above a perfectly reflecting surface. Such a structure has a theoretical absorption of 100 percent at the design wavelength.

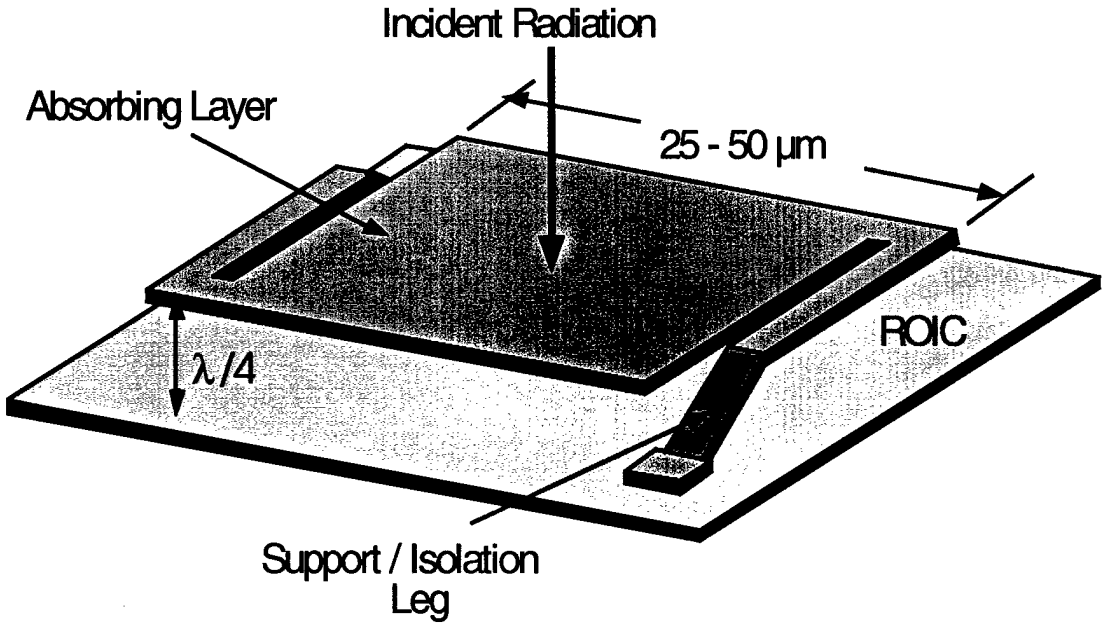

Figure 1: Typical thermal detector structure

In an actual uncooled focal plane array (FPA), the metallized surface of the readout integrated circuit (ROIC) acts as the reflecting surface, and the bolometric or ferroelectric material is formed into a thin sheet spaced about 3 μm above the ROIC to form the quarter-wavelength cavity. Typical pixel pitch in current uncooled focal plane arrays (FPAs) is 50 μm, with a decrease to 25 μm anticipated in the next generation. Since this is only two to three wavelengths of the 8-14 μm light in the long wavelength infrared (LWIR) band, significant small-pixel effects are expected.

The supporting legs can also affect optical absorption in small pixels. This is especially true when the legs are positioned under the absorbing element in an attempt to increase the fill factor. In that case, the legs are inside the optical cavity.
A one-dimensional transfer matrix method was previously used to compute the absorption properties of large (infinite) pixels [3]. That model was used to predict the variation of absorption with cavity thickness and absorber conductance. Use of FDTD also permits calculation of small-pixel and leg effects.

In this study, we were primarily interested in modeling the generic effects of pixel pitch and fill factor, so we have approximated the absorbing detector layer as a two-dimensional conducting sheet spaced one quarter wavelength over a perfectly conducting backplane. This suppressed effects related to the finite thickness of the detector as well as the supporting legs. The previous one-dimensional modeling [3] showed that this is a reasonable approximation, although the detailed layer structure of the absorbing layer could easily be included in FDTD calculations for specific structures.

III. FDTD Model

The FDTD method was first introduced by Yee in his 1966 seminal paper [4]. The method was later refined by Taflove and others [5,6,7] and is now one of the most widely used numerical techniques for solving electromagnetic (EM) problems. The method is extremely general in the materials and geometries it can analyze. Structures that contain inhomogenous, lossy or even anisotropic material properties can be easily handled

The FDTD method derives its name from a direct finite difference approximation to Maxwell's time-dependent curl equations.

$$\frac{\partial \vec{H}}{\partial t} = -\frac{1}{\mu}\nabla \times \vec{E}, \frac{\partial \vec{E}}{\partial t} = \frac{1}{\varepsilon}\nabla \times \vec{H} - \frac{\sigma}{\varepsilon}\vec{E} \qquad (1)$$

Yee's basic scheme is to use a series of finite-difference approximations to transform Maxwell's equations into a system of six algebraic equations. These equations can then be solved using a simple "leap-frog" algorithm. For a detailed description and derivation of the full 3D FDTD equations the reader is referred to [5].

The unknown field distribution over a finite space is calculated by applying the six FDTD equations to a volumetrically sampled grid of cells called Yee cells. Each edge of a Yee cell may be assigned independent electrical properties, which allows one to model complex objects that consist of lossy, inhomogeneous or anisotropic materials. Figure 2 illustrates how the field components are assigned to a typical unit Yee cell.

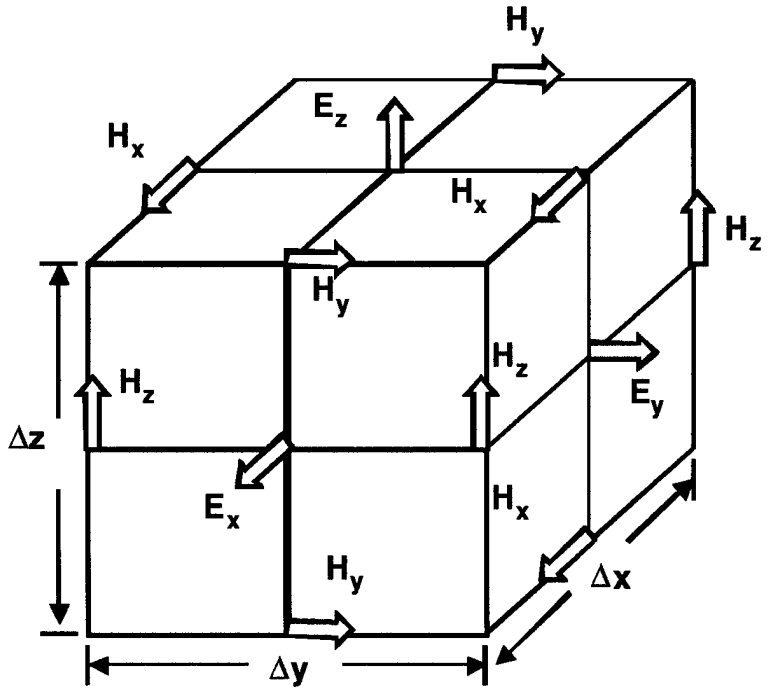

Figure 2: Three dimensional Yee Cell

After incorporating a time-dependent incident field, a time-marching algorithm is employed to calculate the unknown field distribution. At t=0, a plane-wave source of frequency f is assumed to be turned on. Solving the finite-difference equations at all lattice points simulates the propagation of waves from this source. Time stepping continues until the field components at each lattice point reach sinusoidal steady state. Alternatively, non-sinusoidal incident fields that contain an entire band of frequencies (e.g., Gaussian-modulated sinusoids) can be applied. When analyzing structures composed of only linear materials the various frequencies of the incident field propagate independently through the FDTD solution space. Therefore, application of a Fourier Transform to the time-dependent fields at each point in the solution space yields the steady-state field solution throughout the entire frequency spectrum of the incident field. In other words, we can obtain the entire long wavelength response (8-14 μm) of a bolometer array in a single FDTD run.

All calculations were performed using custom FDTD code that contains features that are not commonly found in other EM codes. These include the ability to exploit inherent symmetries found in some of the more common IR detectors. For instance, the bolometer model used here possesses a four fold symmetry that when exploited can significantly reduce the computational complexity of the problem. They also include the ability to simulate infinite periodic arrays by selecting appropriate boundary conditions (BCs).

IV. Summary of Most Important Results

A. *Optical Absorption as a Function of Wavelength*

We used the FDTD model to calculate the fractional absorption (total absorbed power divided by total incident power) of infinite and finite size pixels throughout the long wave IR band (8-14 μm)

1) *Infinite Size Pixel*

We first compared the FDTD result to previous calculations obtained using a transfer-matrix approach used for infinite pixels [3]. The purpose of these calculations was to validate the FDTD model using an independent analytical model and to refine the FDTD parameters (cell size, time step, material properties) to be used in the finite-pixel size calculations. The structure consisted of a conducting sheet with sheet conductivity of $1/Z_0$, where $Z_0 = 120\pi\Omega$ is the impedance of free space, spaced 2.5 μm above a perfectly conducting surface (λ/4 cavity at a 10 μm. freespace wavelength). Periodic BCs were used in the FDTD runs to simulate an infinite pixel. Such a structure has a theoretical absorption of 100 percent at a wavelength of 10 μm.

Figure 3 shows the computed spectral absorption for normally incident light. Note that the FDTD result for the two smaller grid sizes is very close to the analytical (transfer matrix) result. Based on this result, we used a grid size of 0.25 μm for the remainder of the calculations reported here.

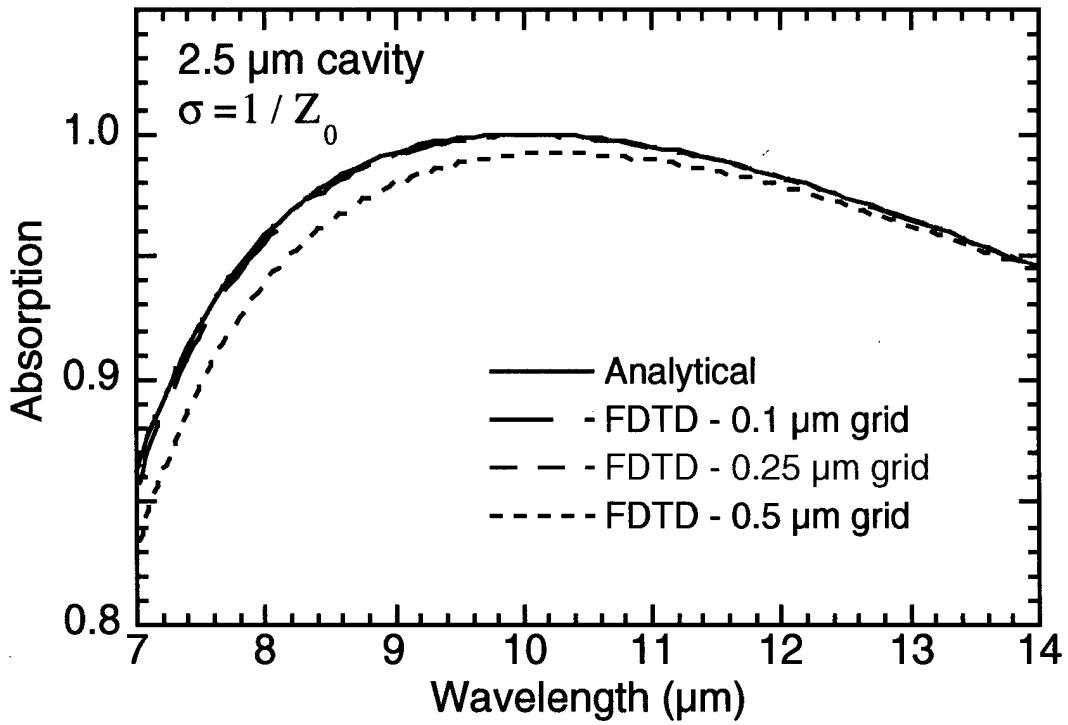

Figure 3: Spectral absorption computer using analytical (transfer matrix) method and using FDTD with three cell sizes.

2) Finite Size Pixel

A series of pixels were run that consisted of a square detector centered within a larger square unit cell. Periodic BCs were applied at the sides so that the detector was implicitly embedded in a periodic array of other identical detectors as in a focal plane array (FPA). The fill factor, *F*, of each pattern was defined as the fraction of area in the unit cell occupied by the detector. Figure 4 shows the calculated absorption for several finite geometries compared with the infinite-pixel result. We expect the fractional absorption, σ_{frac}, to be approximately linearly dependent on *F*, i.e., $\sigma_{frac} = \eta F$, where η is a normalized absorption. However, a plot of the effective η versus wavelength, Figure 3, shows that η is larger in the finite, 25-μm period pixels than in the infinite pixel. This implies that absorption decreases more slowly than detector area, i.e. that the effective optical area of the detector is somewhat larger than its physical area.

B. Optical Coupling Efficiency

To better quantify the expected performance of an uncooled bolometer array we define a quantity, ξ, we call the optical coupling efficiency. This term integrates the fractional absorption over the long wave IR band (8-14 μm) normalized by the black body spectrum. Mathematically ξ is written as

$$\xi = \frac{\int_{\lambda=7\,\mu m}^{\lambda=14\,\mu m} \sigma_{frac}(\lambda) BB(\lambda) d\lambda}{\int_{\lambda=7\,\mu m}^{\lambda=14\,\mu m} BB(\lambda) d\lambda} \qquad (2)$$

where BB(λ) denotes the black body spectrum.

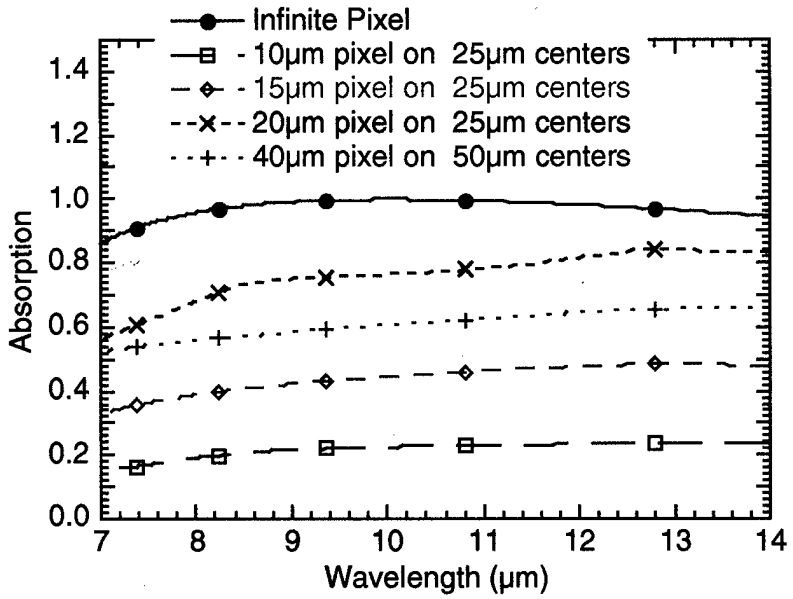

Figure 4: Absorption for finite and infinite pixels

1) Variation with Pixel Size and Fill Factor

We calculated the optical coupling efficiency of pixels ranging in size from 10-50 μm and area fill factors varying from 0-100%. The results are summarized in Figure 5. Without considering diffraction effects the coupling efficiency would vary linearly with area fill-factor. This is purely a consequence of the linear increase in surface area. However, it is clear from Figure 5, that the coupling efficiency variation is far from linear. This is especially true for the smaller 10-20μm pixels. Diffraction effects actually improve the coupling efficiency by bending light incident outside the physical detector surface into the cavity region allowing it to be absorbed after reflection. The optical area of the detector is thus larger than the physical area. For smaller

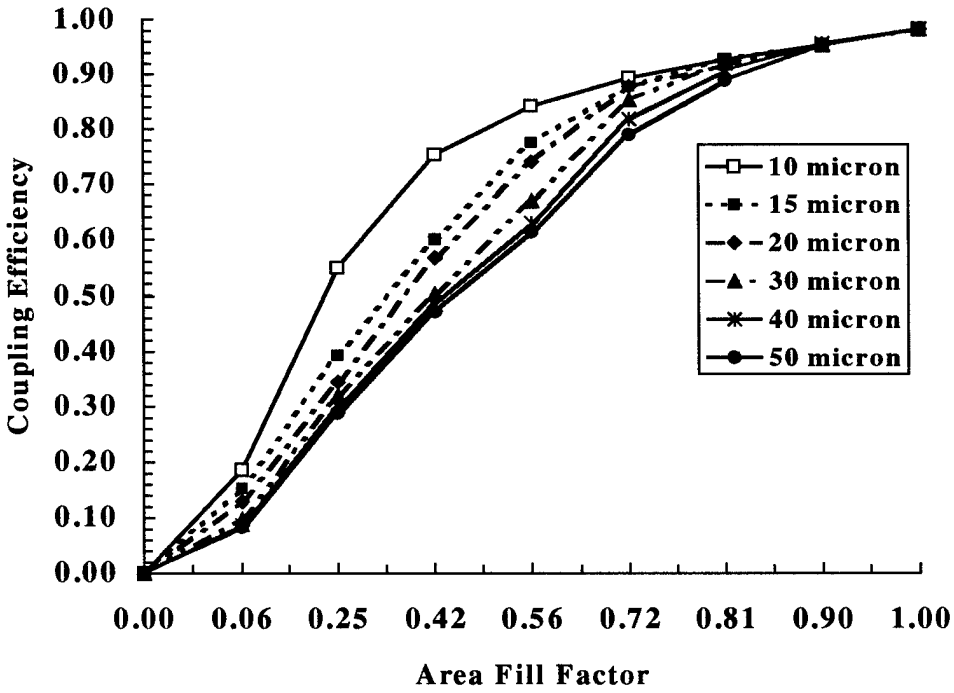

Figure 5. Coupling Efficiency vs Fill Factor for pixel pitches varying from 10-50 μm

pixels this increase in optical area plays a more significant role in the total coupling efficiency (diffraction + geometry) than for larger pixels. To obtain a better understanding of this effect we calculated the absorption pattern of pixels ranging in size from 10-50 μm at a single wavelength (10 μm). Image plots of these absorption patterns are shown in Figure 6. Without diffraction effects one would expect a uniform absorption of energy throughout the entire detector area. For the case of the largest pixel (50 μm) in Figure 6 this is nearly the situation except for some increased absorption at the edges and corners of the detector. However, as the detector size decreases the absorption pattern becomes highly non-uniform indicating a more significant contribution from diffraction.

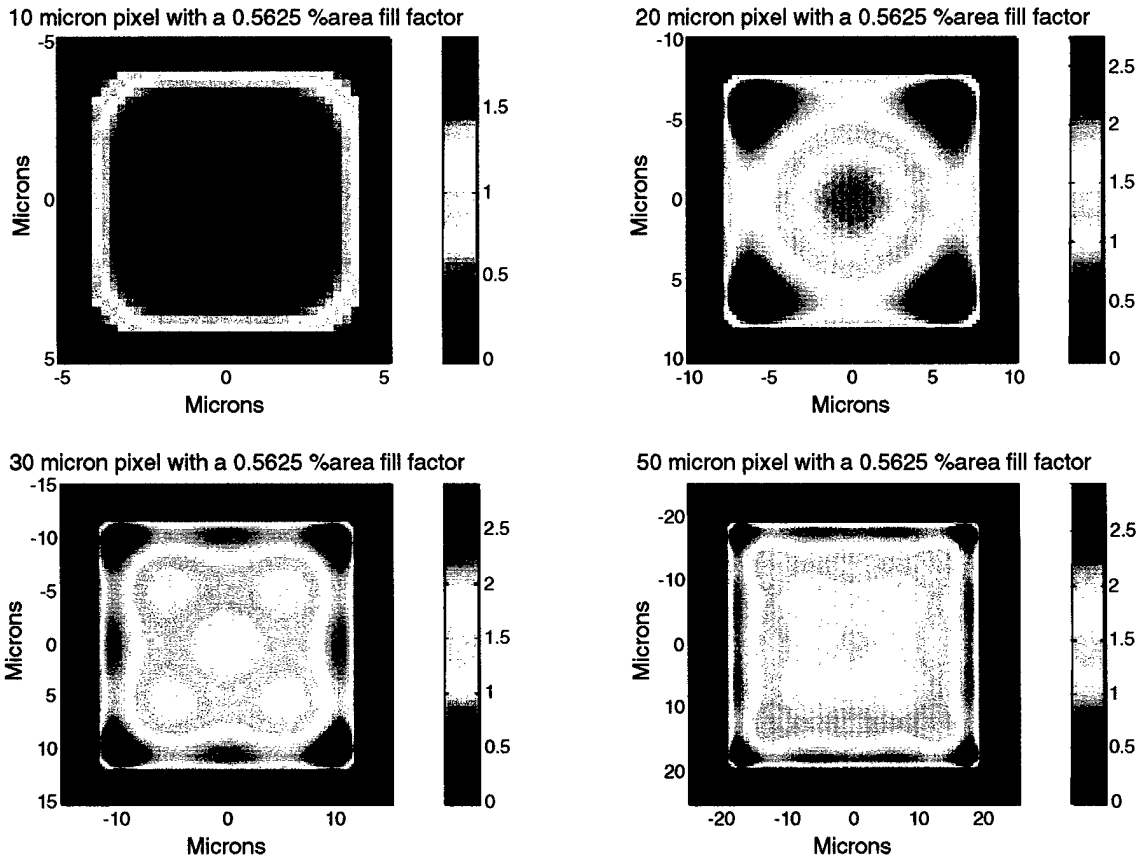

Figure 6: Absorption patterns for incident radiation at a 10μm wavelength

C. Image Performance Model Function

The coupling efficiency shown in Figure 6 includes the geometric effects of a reduced fill factor. The geometric effects are included in most imaging system performance models, so we normalize these results to include only the coupling efficiency due to diffraction. The results are shown in Figure 7. The data from the rigorous models are shown as points. Note that when the pixel pitch is reduced to 10 μm with a small fill factor, diffraction can increase the flux gathering capabilities of the detector by a factor of 3 above the geometric estimate of flux gathering capabilities. Even with a reasonable fill factor of 42 percent, the 10 μm detector pitch obtains 1.8 times the geometric approximation of flux absorption.

The data points were fit using a three dimensional curve-fitting program, where the curve fit was specified to be simple polynomials. A curve fit was obtained with a 0.9844 correlation coefficient and is shown as the mesh surface in figure 7. The equation for the curve fit approximation of diffraction coupling efficiency was

$$\eta_{diffraction} = 0.957 - 1.50\alpha + 26.10/\delta + 4.36\alpha^2 - 39.50/\delta^2 - 47.58\alpha/\delta - 2.883\alpha^3 + 216.3/\delta^3 - 4.414\alpha/\delta^2 + 23.94\alpha^2/\delta \quad (3)$$

where α was the fill factor and δ was the pixel pitch (micrometers). This equation allows the straightforward calculation of diffraction efficiency for the longwave microbolometer as a function of detector pitch and fill factor. This equation can be used without the requirement for a rigorous electromagnetic model as long as it is used within the 8 to 14 μm bandwidth and the

geometry described above. This efficiency model can be included in infrared imaging system performance estimates to account for the effects of diffraction coupling.

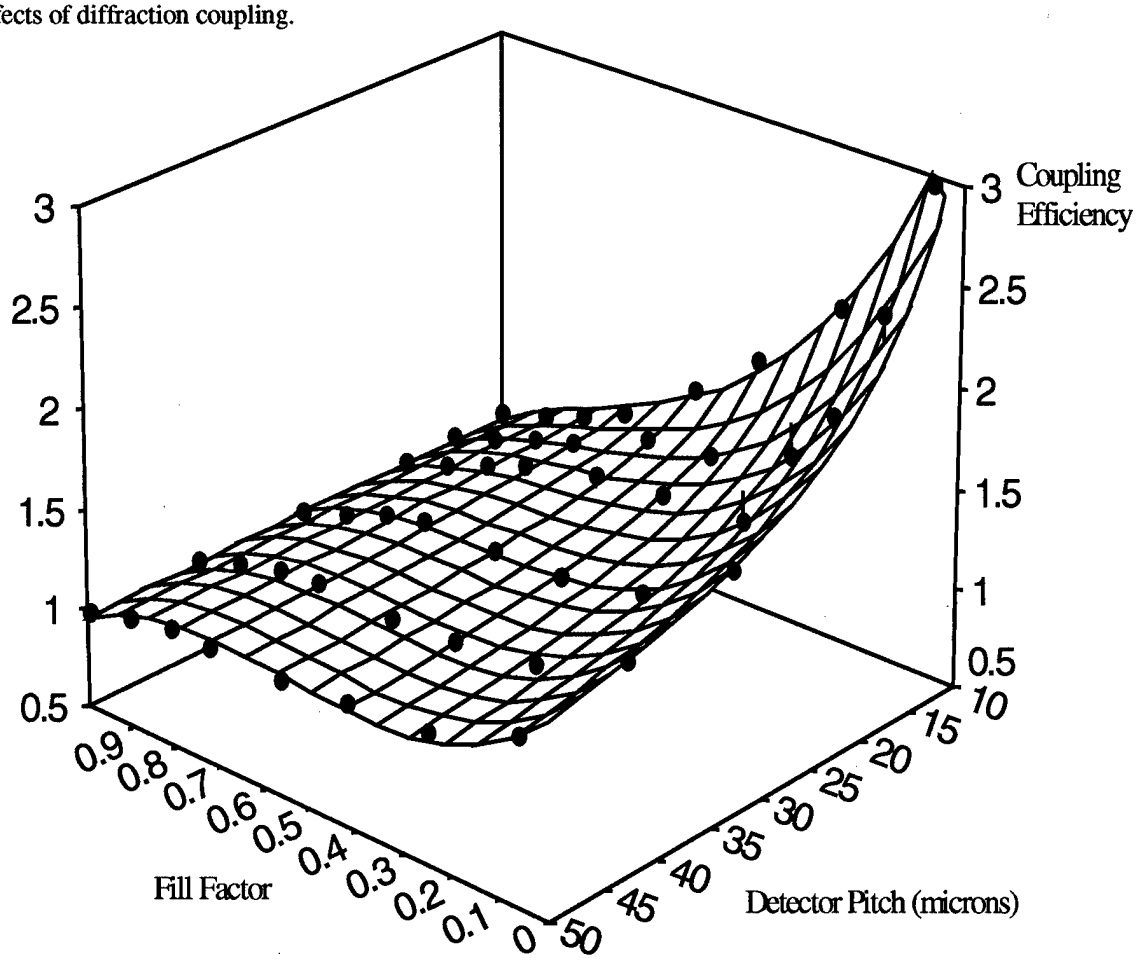

Figure 7: Coupling efficiency due only to diffraction (excludes geometric effects) as a function of detector pitch and fill factor.

To summarize the results, in this project we modeled the optical absorption of uncooled bolometers using a rigorous three dimensional electromagnetic model (FDTD). The model incorporated diffraction as well as geometrical effects and quantified their relative contribution as a function of the pixel's pitch and area fill factor. The results indicated that diffraction tends to improve the flux gathering capability of a pixel beyond what was predicted using simple geometrical models currently employed in most imaging system performance models. This effect is more significant as the pixel size is reduced to only a few optical wavelengths. We also generated a image performance model function that can be used to include diffraction effects in systems level modeling.

V. List of all publications and technical reports

A manuscript entitled, "Rigorous Electromagnetic Analysis of Microbolometer Arrays using the Finite Difference Time Domain Method" is being submitted to Optics Letters. A copy of the manuscript is attached to this report.

VI. Scientific Personnel

a) Uyen Nguyen - Graduate Research Assistant to Dr. Mark Mirotznik at The Catholic University of America progress is being made towards a Ph.D. in electrical engineering.
b) Dr. Mark Mirotznik, Associate Professor at The Catholic University of America - Principal Investigator
c) Dr. Dennis Prather, Associate Professor at The University of Delaware - Co-Principal Investigator
d) Dr. William Beck, Senior Scientist at The Army Research Laboratories, Adelphi MD

e) Dr. Ron Driggers, Army Night Vision Laboratory
f) Dr. Richard Vollmerhausen, Army Night Vision Laboratory

VII. Report of Inventions

None

VIII. BIBLIOGRAPHY

[1] A. D. Parsons and D. J. Pedder, "Thin-film infrared absorber structures for advanced thermal detectors," *J. Vac. Sci. Technol. A* **6**, pp. 1686-1689, 1988.

[2] V. T. Bly and T. Cox, "Infrared absorber for ferroelectric detectors," *Appl. Opt.* **33**, pp. 26-30, 1994.

[3] W. A. Beck, et al., "Infrared absorption by ferroelectric thin-film structures," IRIS Materials Group (ERIM, Monterey, 1998),

[4] K. S. Yee, "Numerical solution of initial boundary value problems involving Maxwell's equations in isotropic media," *IEEE Trans. Antennas Propagat.* **AP-14**, pp. 302-307, 1966.

[5] A. Taflove, "Computational Electrodynamics: The Finite-Difference Time-Domain Method," *CRC Press*, Boton Raton, 1993

[6] R. Luebbers, R., F. Hunsberger, K. Kunz, R. Standler, and M. Schneider, "A frequency-dependent finite-difference time-domain formulation for dispersive materials," *IEEE Trans. Electromagnetic Compatibility*, vol 32, 1990, pp. 222-229

[7] J. Berenger, "A perfectly matched layer for the absorption of electromagnetic waves," *J. Computational Physics*, vol. 4, 1994, pp. 268-270

VIII. APPENDICES

None